Spatial distributions of railway-generated ground vibrations at and around sleeper passage frequencies

Victor V. Krylov

Department of Aeronautical and Automotive Engineering,
Loughborough University,
Loughborough, Leicestershire LE11 3TU, UK

Abstract

In this paper, spatial distributions of ground vibrations generated by railway trains travelling at conventional speeds on straight tracks are investigated theoretically. The main attention is being paid to calculations of spatial distributions of ground vibrations generated by a single axle load at and around sleeper passage frequencies that are defined by train speeds and sleeper periodicity. It is demonstrated that, at sleeper passage frequencies, generated ground vibrations represent plane waves propagating symmetrically away from the track in the normal directions to it. At frequency components that are slightly above or below sleeper passage frequencies, generated ground vibrations still remain plane waves, but they are now propagating at certain angles in respect of the normal directions to the track.

1. Introduction

Over the last decades, high-speed railways underwent rapid development throughout the world. As many other means of transportation, high-speed railways encounter a number of environmental problems. In particular, ground vibrations, mostly Rayleigh surface waves, generated by high-speed trains is one of the major environmental problems that must be mitigated to allow high-speed trains to be used in densely populated areas (see e.g. the recent book [1]).

The intensity of railway-generated ground vibrations generally becomes larger at higher train speeds. The increase in amplitudes of generated ground vibrations can be especially large when train speeds approach the velocity of Rayleigh surface wave in the supporting ground. As was theoretically predicted by the present author [2-5], if a train speed v exceeds the Rayleigh wave velocity c_R in the supporting soil, a *ground vibration boom* occurs. This phenomenon is similar to a sonic boom from supersonic aircraft, and it is associated with a very large increase in generated ground vibrations, as compared to the case of conventional trains. The existence of ground vibration boom at trans-Rayleigh train speeds has been later confirmed experimentally [6, 7].

The increased attention to the problems of ground vibrations from high-speed trains is reflected in a growing number of theoretical and experimental investigations in this area (see e.g. [8-27]). In addition to ground vibration problems typical for trains approaching or exceeding Rayleigh wave velocity in the ground, there are also many problems associated with trains travelling at lower (conventional) train speeds. In particular, for the important case of generation of ground vibrations at the so-called sleeper passage frequencies, very little or no research into the structure and directions of generated waves has been carried out so far.

The aim of the present paper is to investigate spatial distributions of ground vibrations generated at and around sleeper passage frequencies by high-speed trains travelling at conventional speeds, i.e. at speeds not exceeding Rayleigh wave velocity in the supporting ground. It will be demonstrated that spatial distributions of generated Rayleigh waves in this case can change significantly, depending on train speeds, frequency components, and distance between adjacent sleepers.

2. Theoretical background

The main mechanisms of railway-generated ground vibrations are the wheel-axle pressure onto the track, the effects of joints in unwelded rails, the dynamically induced forces of carriage- and wheel-axle vibrations excited due to random roughness of wheels and rails, as well as variations in sleeper-ground contact from sleeper to sleeper. In this paper we limit our consideration with only the first mentioned generation mechanism, which is always present, even for ideally flat rails and perfectly round wheels – namely, the quasi-static pressure of wheel axles acting onto the track. This universal generation mechanism is responsible for the above-mentioned railway-generated ground vibration boom, and it is also responsible for ground vibrations generated at sleeper passage frequencies considered in this paper. It should be noted that at other frequencies the unevenness of real wheels and rails usually plays a dominant role in generation of ground vibrations (see e.g. [14, 15, 18-20]).

The quasi-static pressure generation mechanism results from load forces applied to the railway track from each wheel axle. These load forces cause downward deflections of the track that are moving together with the loads, thus producing a wave-like motion along the track at speed of the train, which results in a distribution of each axle load over all the rail sleepers that are within the track deflection distance. Each sleeper, in turn, acts as a vertical force applied to the ground during the time necessary for a deflection curve to pass through the sleeper. These vertical forces can be approximately considered as point forces applied to the ground's surface, assuming that shortest wavelengths of generated ground vibrations are still essentially larger than sleeper dimensions. To determine the track deflection curve and thus the time dependence of the forces applied from each sleeper to the ground the system of track and ground is modelled as an Euler-Bernoulli beam resting on Winkler foundation.

According to the earlier developed general theory [2-5, 9-11], in order to calculate ground vibrations generated by a train due to the quasi-static pressure mechanism, one needs to take into account the superposition of waves generated by each elementary source of ground vibrations (sleeper) activated by wheel axles of all carriages, with the time and space differences between sources (sleepers) being taken into account. In doing so we take into account only the contribution of generated Rayleigh surface waves, because they make the main contribution to ground vibrations causing environmental problems.

Being interested in fundamental features of railway-generated Rayleigh waves, in this paper, for the sake of simplicity, we will consider ground vibrations generated by a single axle load only. In this case, we can use the following expression for the vertical vibration velocity v_z of Rayleigh waves generated on the ground surface ($z = 0$) at the point of observation having the coordinates x, y by a single axle load moving along the straight track (located on the x-axis) at constant speed v (see e.g. [9-11]):

$$v_z(x,y,\omega) = P(\omega)D(\omega)\sum_{n=-\infty}^{\infty}\frac{1}{\sqrt{\rho_n}}\exp\left[i\frac{\omega}{v}nd + (i-\gamma)\frac{\omega}{c_R}\rho_n\right]. \qquad (1)$$

Here ρ_n is the distance from each sleeper characterised by a number n to the point of observation, ω is a circular frequency, v is the train speed, d is a sleeper periodicity, c_R is the Rayleigh wave velocity, and $\gamma = 0.001 - 0.1$ is a non-dimensional loss factor describing the attenuation of Rayleigh waves in soil.

The function $P(\omega)$ in Equation (1) represents the Fourier spectrum of a force acting from each sleeper to the ground. The expression for $P(\omega)$ has the form (see [5, 10, 11] for detail):

$$P(\omega) = -\frac{12.8\dfrac{Td}{v\pi^2}}{\dfrac{\omega^4}{\beta^4 v^4} - 4\dfrac{\omega^2}{c_{\min}{}^2\beta^2} - 8i\dfrac{\eta\omega}{c_{\min}\beta} + 4}, \qquad (2)$$

where T is the axle load, c_{min} is the minimal phase velocity of track flexural waves propagating in a track/ground system (this velocity is related to c_R via the parameters of Winkler foundation expressed in terms of the ground elastic parameters, and it is usually larger than c_R by 10-20 %), β is the parameter dependent on the elastic properties of track and ground [10] and measured in m^{-1}, and η is a non-dimensional track damping parameter. For relatively low train speeds, i.e., for $v < c_R$, the 'dynamic' solution (2) for the force spectrum $P(\omega)$ goes over to the quasi-static one [10, 11]. When train speeds increase and approach or exceed the minimal track wave velocity c_{min}, the spectra $P(\omega)$ become broader and larger in amplitudes, and a second peak appears at higher frequencies.

The function $D(\omega)$ in Equation (1) has the form

$$D(\omega) = \frac{(-i\omega)qk_R{}^{1/2}k_t{}^2}{(2\pi)^{1/2}\mu F'(k_R)}\exp(-i\frac{3\pi}{4}), \qquad (3)$$

where the factor $F'(k_R) = [dF(k)/dk]|_{k=kR}$ is a derivative of the Rayleigh determinant

$$F(k) = (2k^2 - k_t{}^2)^2 - 4k^2(k^2 - k_t{}^2)^{1/2}(k^2 - k_l{}^2)^{1/2} \qquad (4)$$

taken at $k = k_R$. Here $k_R = \omega/c_R$ is the wavenumber of a Rayleigh surface wave, $k_l = \omega/c_l$ and $k_t = \omega/c_t$ are the wavenumbers of longitudinal and shear bulk elastic waves, where $c_l = [(\lambda + 2\mu)/\rho_0]^{1/2}$ and $c_t = (\mu/\rho_0)^{1/2}$ are longitudinal and shear wave velocities, λ and μ are the elastic Lame′ constants, ρ_0 is mass density of the ground, and $q = (k_R^2 - k_l^2)^{1/2}$.

The analysis of the Equation (1) shows that maximum radiation of ground vibrations takes place if the train speed v is larger than Rayleigh wave velocity c_R [2-5, 9-11] (such trains are often called 'trans-Rayleigh trains'). Under this condition, a *ground vibration boom* takes place, i.e., ground vibrations are generated as quasi-plane Rayleigh surface waves symmetrically propagating at angles $\Theta = cos^{-1}(c_R/v)$ in respect to the track, and with amplitudes much larger than in the case of conventional trains. This phenomenon is similar to the well-known phenomenon of *sonic boom* from supersonic aircraft.

It should be noted that for trans-Rayleigh trains these symmetrically propagating Rayleigh surface waves are generated equally well on tracks with and without railway sleepers, whereas for conventional (sub-Rayleigh) trains the presence of sleepers for the possibility of generation of Rayleigh waves is paramount. Without them no propagating waves are generated by a force moving at constant sub-Rayleigh speeds in the framework of the quasi-static pressure generation mechanism. Only quasi-static localised displacements are present in this case that are moving along with the force. However, if the same force is moving along a railway track supported by discrete sleepers, Rayleigh waves are generated even at sub-Rayleigh load speeds. For a single moving load, the efficient generation takes place mainly at and around the so-called sleeper passage frequencies $f_{sp}^{(m)} = m(v/d)$, where v is the load speed, d is the sleeper periodicity, and m = 1, 2, 3... . In this paper, we will be interested in spatial distributions of ground vibrations (Rayleigh surface waves) generated by a single moving load at and around sleeper passage frequencies.

3. Numerical calculations and discussion

In what follows, we describe the results of the calculations of spatial distributions of railway-generated ground vibration fields $v_z(x,y, \omega)$ (i.e. wave snapshots shown in arbitrary linear units) over a certain surface area with a railway track in the middle of it (located along the x-axis) for some interesting situations corresponding to frequency components at and around sleeper-passage frequencies. Calculations have been carried out according to Equations (1)-(4) over the surface area of 40×40 m to obtain spatial distributions of ground vibrations (Rayleigh waves) generated at different frequency components f by a single axle load travelling along a straight railway track at speeds v. The summation in Equation (1) has been taken over 120 sleepers in all cases for each point of observation, and the magnitude of the axle load has been considered to be the same in all cases. The results will be presented as greyscale contour plots. It will be assumed that the velocity of Rayleigh waves in the ground is $c_R = 80\ m/s$ for all cases. Other relevant parameters are as follows: $d = 0.7\ m$, $\beta = 1.28\ m^{-1}$, which is typical for British railway tracks, and $\gamma = 0.001$.

It is instructive to start with the distinctive case of ground vibrations generated by a single axle load travelling at a trans-Rayleigh speed $v > c_R$, which is associated with generation of ground vibration boom by high-speed trains. Because the amplitudes of generated ground vibrations are the largest in this case, the obtained results can be used as a useful reference for comparison with ground vibrations generated at lower (conventional) train speeds.

Figure 1 illustrates the results of such calculations at $f = 11$ Hz as a contour plot for an axle load travelling at the trans-Rayleigh speed $v = 90$ m/s (this gives the value of Mach number $M = v/c_R = 1.125$). The horizontal and vertical axes in Fig. 1 represent surface rectangular coordinates in normalised (non-dimensional) units changing from -1 to 1: $x_{norm} = x[m]/20[m]$ and $y_{norm} = y[m]/20[m]$. The direction of the load motion is from left to right.

As it can be seen from Fig. 1, the spatial distribution of ground vibrations (Rayleigh waves) shows a typical picture of plane waves generated symmetrically in respect of the track at Mach angles $\Theta = cos^{-1}(c_R/v)$. It should be noted that Mach angles do not depend on frequency in the case under consideration. Therefore, for the same trans-Rayleigh speed, ground vibrations will be generated at the same Mach angles for any frequency components.

The amplitudes of generated ground vibrations (in arbitrary linear units) can be estimated from the surface plot corresponding to Fig. 1 (not shown here for shortness). The vertical scale in this surface plot gives the range of vertical components of ground vibration velocities between -1.551 and 1.819, which can be compared with the amplitudes of ground vibrations generated at sub-Rayleigh speeds that will be calculated below.

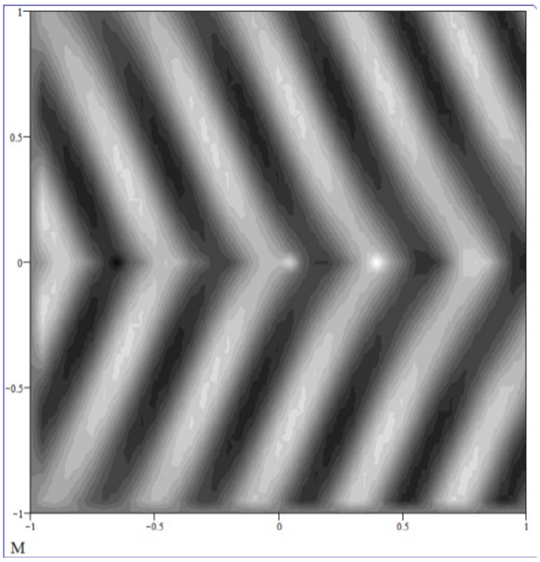

Fig. 1. Spatial distribution of ground vibrations over the surface area 40 x 40 m generated at the frequency component $f = 11$ Hz by a single axle load travelling at speed $v = 90$ m/s.

Let us now consider generation of ground vibrations by a single axle load travelling at conventional (sub-Rayleigh) speeds $v < c_R$. In particular, let us assume that $v = 14$ m/s (or 50.4 km/h), and consider spatial distribution of generated ground vibrations at the first sleeper passage frequency $f_{sp}^{(1)} = (v/d) = 14/0.7 = 20$ [Hz]. The results are shown in Fig. 2.

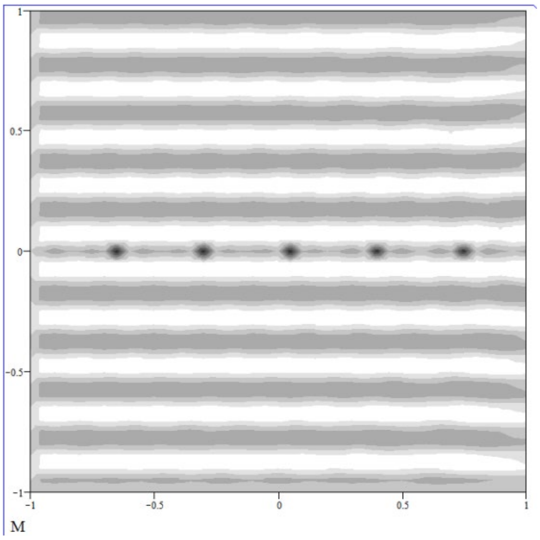

Fig. 2. Spatial distribution of ground vibrations over the surface area 40 x 40 m generated at the frequency component $f = 20$ Hz (first sleeper passage frequency) by a single axle load travelling at speed $v = 14$ m/s.

As it can be seen from Fig. 2, the spatial distribution of ground vibrations generated by a single load at the first sleeper passage frequency represents plane waves propagating symmetrically away from the track in the normal directions to it. This is due to the fact that at sleeper passage frequencies all sleepers are radiating in phase. The amplitudes of generated ground vibrations here (in arbitrary linear units) can be also estimated from the surface plot corresponding to Fig. 2 (not shown here). The vertical scale in the surface plot in this case gives the range of vertical components of vibration velocities between -0.031 and 0.009, which demonstrates that the amplitudes of generated Rayleigh waves in this case are roughly by 85 times smaller than in the case of generation of ground vibration boom by a single load illustrated in Fig. 1.

Distribution of ground vibrations generated by the same single axle load at the frequency component $f = 21$ Hz, which is slightly above the first sleeper passage frequency for this case, is shown in Fig. 3. One can see that the wave fronts in this case change symmetrically their directions of propagation from the normal directions to the track, as in the case of the first sleeper passage frequency (see Fig. 2), to the directions that are slightly deflected from the normal directions. The reason for this deflection is the phase differences between vibrating sleepers at this frequency. The amplitudes of generated ground vibrations in this case are roughly the same as in Fig. 2.

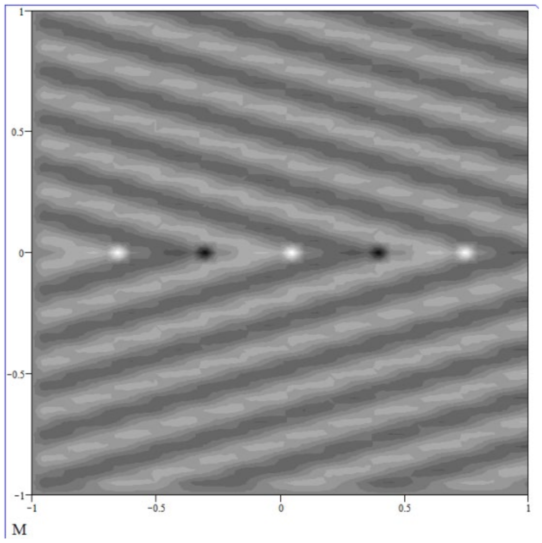

Fig. 3. Spatial distribution of ground vibrations over the surface area 40 x 40 m generated at the frequency component $f = 21$ Hz (slightly above the first sleeper passage frequency) by a single load travelling at speed $v = 14$ m/s.

For even higher frequency component $f = 23$ Hz, the ground vibrations generated by the same single axle load undergo further evolution, as shown in Fig. 4. It can be seen that the directions of propagation of the wave fronts in this case deflect symmetrically even further from the normal directions to the track, and the amplitudes of generated ground vibrations in this case are roughly the same as in Figs. 2 and 3.

It should be noted that spatial distributions of ground vibrations in Figs. 3 and 4 look similar to that shown in Fig.1 for the case of ground vibration boom. One should remember though that the associated physical mechanisms are absolutely different. Rayleigh wave radiation by a load travelling at sub-Rayleigh speeds illustrated in Figs. 3 and 4 is entirely due to the presence of sleepers. Therefore, radiation angles of generated waves depend here on frequency and on sleeper periodicity, as it follows from the comparison of Figs. 3 and 4.

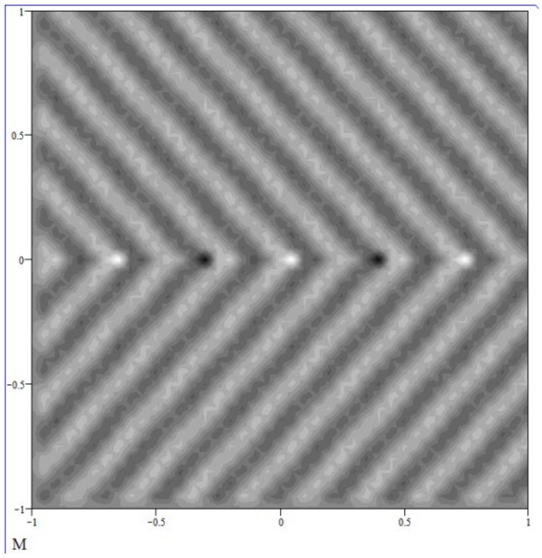

Fig. 4. Spatial distribution of ground vibrations over the surface area 40 x 40 m generated at the frequency component f = 23 Hz (above the first sleeper passage frequency) by a single axle load travelling at speed v = 14 m/s.

Let us now consider ground vibrations generated by the same moving load at the frequency component f = 19 Hz, which is slightly below the first sleeper passage frequency. The resulting spatial distribution of generated ground vibrations (Rayleigh waves) is shown in Fig. 5. The noticeable difference from the previous figures can be seen in the directions of propagation of generated ground vibrations. These directions are now deflected symmetrically in the opposite directions from the normal directions to the track, in comparison with Figs. 3 and 4, so that horizontal components of the corresponding wave vectors become negative, i.e. their direction (from right to left) is now opposite to the direction of the load motion (from left to right).

Figure 6 shows the spatial distribution of ground vibrations generated by the same axle load at the lower frequency component f = 18 Hz. It can be seen that ground vibrations in this case represent slightly distorted plane waves that propagate at larger angles in respect of the normal directions to the track.

For even lower frequency component, f = 17 Hz, some changes in the spatial distribution of generated ground vibrations become obvious, as can be seen from Fig. 7. Namely, the generated Rayleigh waves cease to be plane and become cylindrical, which indicates the end of constructive interference between waves generated by different sleepers for frequency components that are far away enough from the sleeper passage frequencies. The amplitudes of generated ground vibrations are further reduced in this case, as it can be expected from consideration of the frequency spectra of generated ground vibrations at the sides of the frequency peaks associated with sleeper passage frequencies.

Thus, resuming the above, it can be concluded that ground vibrations at and around the first sleeper passage frequency are generated as plane waves that are steering around the normal directions to the track either in the direction of the load motion - for higher frequencies, or in the opposite direction - for lower frequencies. Such a behaviour is very similar to the behaviour of electromagnetic 'travelling-wave antennas' used in microwave technology.

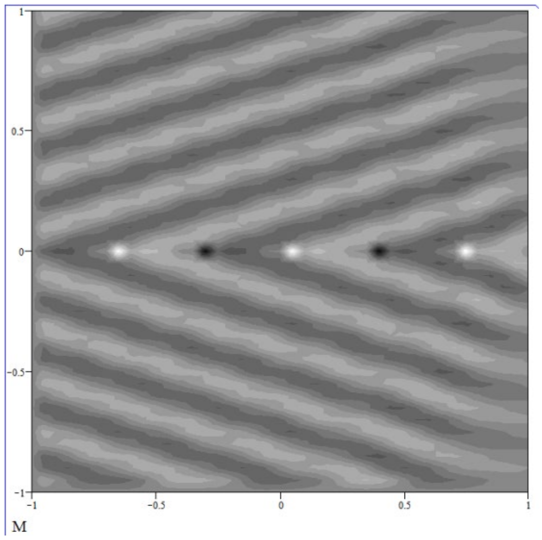

Fig. 5. Spatial distribution of ground vibrations over the surface area 40 x 40 m generated at the frequency component $f = 19$ Hz (slightly below the first sleeper passage frequency) by a single load travelling at speed $v = 14$ m/s.

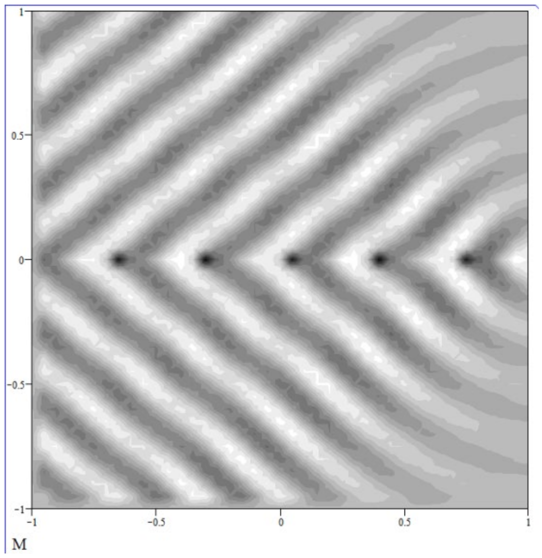

Fig. 6. Spatial distribution of ground vibrations over the surface area 40 x 40 m generated at the frequency component $f = 18$ Hz (below the first sleeper passage frequency) by a single axle load travelling at speed $v = 14$ m/s.

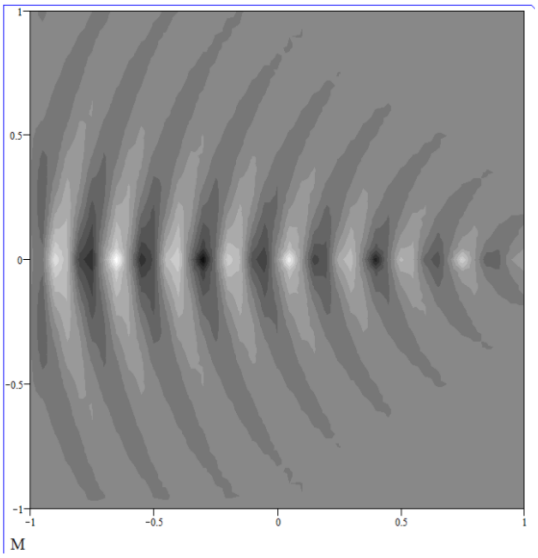

Fig. 7. Spatial distribution of ground vibrations over the surface area 40 x 40 m generated at the frequency component $f = 17$ Hz (below the first sleeper passage frequency) by a single axle load travelling at speed $v = 14$ m/s.

So far we discussed ground vibrations generated at and around the first sleeper passage frequency $f_{sp}^{(1)} = (v/d) = 20$ [Hz]. It can be shown that for the second sleeper passage frequency $f_{sp}^{(2)} = 2(v/d)$, which is equal to 40 Hz in the case under consideration, the situation is very similar. This is illustrated by Fig. 8 showing the spatial distribution of generated ground vibrations by the same moving load at the frequency component $f = 40$ Hz.

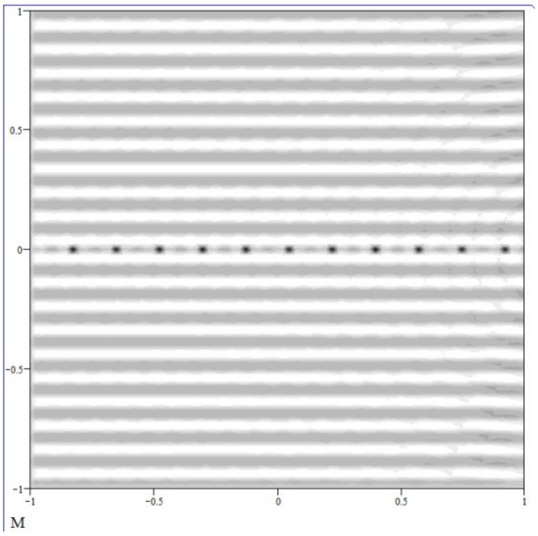

Fig. 8. Spatial distribution of ground vibrations over the surface area 40 x 40 m generated at the frequency component $f = 40$ Hz (second sleeper passage frequency) by a single axle load travelling at speed $v = 14$ m/s.

Spatial distributions of ground vibrations generated under the same conditions at the frequency components $f = 42$ Hz and $f = 38$ Hz are shown in Figs. 9 and 10 respectively. Again, one can see opposite changes in directions of plane wave propagation at these frequencies.

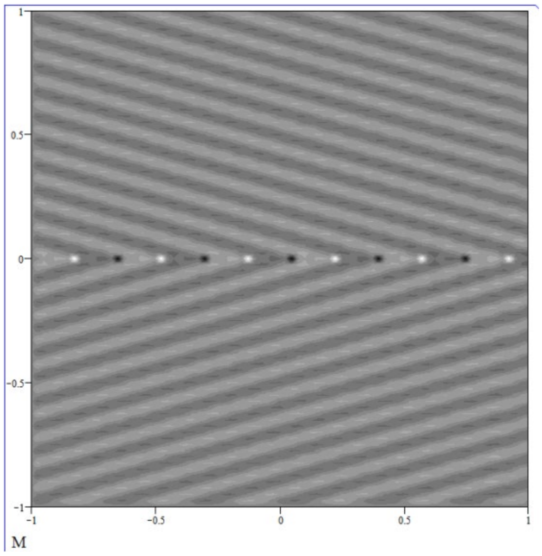

Fig. 9. Spatial distribution of ground vibrations over the surface area 40 x 40 m generated at the frequency component $f = 42$ Hz (above the second sleeper passage frequency) by a single load travelling at speed $v = 14$ m/s.

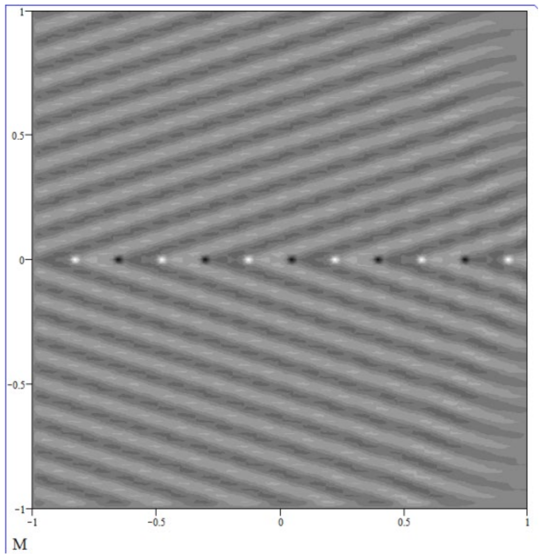

Fig. 10. Spatial distribution of ground vibrations over the surface area 40 x 40 m generated at the frequency component $f = 38$ Hz (below the second sleeper passage frequency) by a single load travelling at speed $v = 14$ m/s.

A similar behaviour can be observed also for the third sleeper passage frequency and for higher order sleeper passage frequencies. However, because of the limited widths of railway-generated ground vibration spectra (usually in the range of 0 - 100 Hz), only a small number of lowest order sleeper passage frequencies can be important.

4. Conclusions

It has been demonstrated in this paper that, at sleeper passage frequencies, railway-generated ground vibrations represent plane waves propagating symmetrically away from the track in the normal directions to it.

At frequencies slightly above or slightly below sleeper passage frequencies, generated ground vibrations still remain plane waves, but their radiation takes place at certain angles in respect of the normal directions to the track. These radiation angles depend on train speed, on frequency and on sleeper periodicity. For frequencies slightly above sleeper passage frequencies, the above-mentioned radiation angles are counted towards the direction of the train (axle load) motion, whereas for frequencies slightly below sleeper passage frequencies, the radiation angles are counted toward the opposite direction.

The above-mentioned properties of railway-generated ground vibrations at and around sleeper passage frequencies could be used for their more efficient observation and monitoring.

References

[1] V.V. Krylov (editor), Ground Vibrations from High-speed Railways: Prediction and Mitigation. ICE Publishing, London (2019).

[2] V.V. Krylov, On the theory of railway-induced ground vibrations, Journal de Physique IV, Vol. 4, No. C5, pp. 769-772 (1994).

[3] V.V. Krylov, Generation of ground vibrations by superfast trains, Applied Acoustics, Vol. 44, pp. 149-164 (1995).

[4] V.V. Krylov, Vibrational impact of high-speed trains. I. Effect of track dynamics, Journal of the Acoustical Society of America, Vol. 100, No. 5, pp. 3121-3134 (1996); Erratum, Vol. 101, No. 6, pp. 3810 (1997).

[5] V.V. Krylov, Effect of track properties on ground vibrations generated by high-speed trains, Acustica - Acta Acustica, Vol. 84, No. 1, pp. 78-90 (1998).

[6] C. Madshus, A.M. Kaynia, High speed railway lines on soft ground: dynamic behaviour at critical train speed, Proc. 6th International Workshop on Railway and Tracked Transit System Noise, Ile des Embiez, France (1998), pp. 108-119.

[7] K. Adolfsson, B. Andreasson, P.-E. Bengtsson, P. Zackrisson, High speed train X2000 on soft organic clay – measurements in Sweden. In: Barends FBJ et al., editors. Proceedings of the 12th European Conference on Soil Mechanics and Geotechnical Engineering. "*Geotechnical Engineering for Transportation Infrastructure*". Amsterdam, The Netherlands, 7-10 June 1999. A.A. Balkema: Rotterdam (1999), Vol. 3. pp. 1713-1718.

[8] X. Sheng, C.J.C. Jones, M. Petyt, Ground vibration generated by a load moving along a railway track, Journal of Sound and Vibration, Vol. 228, No 1, pp. 129–156 (1999).

[9] V.V. Krylov, Ground vibration boom from high-speed trains, Journal of Low Frequency Noise, Vibration and Active Control, Vol. 18, No 4, pp. 207-218 (1999).

[10] V.V. Krylov, A.R. Dawson, M.E. Heelis, A.C. Collop, Rail movement and ground waves caused by high-speed trains approaching track-soil critical velocities, Proceedings of the Institution of Mechanical Engineers, Part F: Journal of Rail and Rapid Transit, Vol. 214, pp. 107-116 (2000).

[11] V.V. Krylov, Generation of ground vibration boom by high-speed trains, in V.V. Krylov (editor), Noise and Vibration from High-speed Trains. Thomas Telford Publishing, London (2001), pp. 251-283.

[12] C. Madshus, A.M. Kaynia, High-speed railway lines on soft ground: dynamic behaviour at critical train speed, Journal of Sound and Vibration, Vol. 231, No. 3, pp. 689-701 (2000).

[13] H. Takemiya, Ground vibrations alongside tracks induced by high-speed trains: prediction and mitigation, in: V.V. Krylov (editor), Noise and Vibration from High-speed Trains, Thomas Telford Publishing, London (2001), pp. 347-393.

[14] G. Degrande, L. Schillemans, Free field vibrations during the passage of a Thalys high-speed train at variable speed, Journal of Sound and Vibration, Vol. 247, No. 1, pp. 131-144 (2001).

[15] X. Sheng, C.J.C. Jones, D.J. Thompson, A comparison of a theoretical model for quasi-statically and dynamically induced environmental vibration from trains with measurements, Journal of Sound and Vibration, Vol. 267, No 3, pp. 621–635 (2003).

[16] H. Takemiya, Simulation of track-ground vibrations due to a high-speed train: the case of X2000 at Ledsgard, Journal of Sound and Vibration, Vol. 261, No 3, pp. 503–526 (2003).

[17] A.V. Vostroukhov, A.V. Metrikine, Periodically supported beam on a visco-elastic layer as a model for dynamic analysis of a high-speed railway track, International Journal of Solids and Structures, Vol. 40, No 21, pp. 5723–5752 (2003).

[18] X. Sheng, C.J.C. Jones, D.J. Thompson, A theoretical study on the influence of the track on train-induced ground vibration, Journal of Sound and Vibration, Vol. 272, pp. 909–936 (2004).

[19] L. Auersch, The excitation of ground vibration by rail traffic: theory of vehicle–track–soil interaction and measurements on high-speed lines, Journal of Sound and Vibration, Vol. 284, pp. 103–132 (2005).

[20] G. Lombaert, G. Degrande, Ground-borne vibration due to static and dynamic axle loads of InterCity and high-speed trains, Journal of Sound and Vibration, Vol. 319, pp. 1036–1066 (2009).

[21] W. Zhai, Z. He, X. Song, Prediction of high-speed train induced ground vibration based on train track-ground system model, Earthquake Engineering and Engineering Vibration, Vol. 9, No 4, pp. 545–555 (2010).

[22] D. Connolly, A. Giannopoulos, M. Forde, Numerical modelling of ground borne vibrations from high speed rail lines on embankments, Soil Dynamics and Earthquake Engineering, Vol. 46, pp. 13–19 (2013).

[23] M. Banimahd, P. Woodward, J. Kennedy, G. Medero, Three-dimensional modelling of high speed ballasted railway tracks, Proceedings of the Institution of Civil Engineers - Transport, Vol. 166, No 2, pp. 113-123 (2013).

[24] G. Kouroussis, D. Connolly, O. Verlinden, Railway induced ground vibrations - a review of vehicle effects, International Journal of Rail Transportation, Vol. 2, No. 2, pp. 69-110 (2014).

[25] Z. Dimitrovová, Analysis of the critical velocity of a load moving on a beam supported by a finite depth foundation, International Journal of Solids and Structures, Vol. 122-123, pp. 128-147 (2017).

[26] V.V. Krylov, Focusing of ground vibrations generated by high-speed trains travelling at trans-Rayleigh speeds, Soil Dynamics and Earthquake Engineering, Vol. 100, pp. 389-395 (2017).

[27] Z. Yuan, Z. Cao, A. Boström, Y. Cai, The influence of pore-fluid in the soil on ground vibrations from a tunnel embedded in a layered half-space, Journal of Sound and Vibration, Vol. 419, pp. 227-248 (2018).